



Laboratory and pilot plant scale study on the electrochemical oxidation of landfill leachate

Ángela Anglada, Ana M. Urriaga, Inmaculada Ortiz*

Departamento de Ingeniería Química y Química Inorgánica, E.T.S.I.I. y T., Universidad de Cantabria, Avenida de los castros s/n, 39005 Santander, Spain

ARTICLE INFO

Article history:

Received 4 March 2010

Received in revised form 11 May 2010

Accepted 15 May 2010

Available online 9 June 2010

Keywords:

Electrochemical oxidation

landfill leachate

change of scale

pilot plant

ABSTRACT

Kinetic data regarding COD oxidation were measured in a laboratory scale cell and used to scale-up an electro-oxidation process for landfill leachate treatment by means of boron-doped diamond anodes. A pilot-scale reactor with a total BDD anode area of 1.05 m² was designed. Different electrode gaps in the laboratory and pilot plant cells resulted in dissimilar reactor hydrodynamics. Consequently, generalised dimensionless correlations concerning mass transfer were developed in order to define the mass transfer conditions in both electrochemical systems. These correlations were then used in the design equations to validate the scale-up procedure. A series of experiments with biologically pre-treated landfill leachate were done to accomplish this goal. The evolution of ammonia and COD concentration could be well predicted.

© 2010 Elsevier B.V. All rights reserved.

1. Introduction

Electrochemical oxidation over boron-doped diamond (BDD) electrodes has received special attention in recent years because it exhibits high treatment efficiencies. BDD electro-oxidation has been successfully applied to eliminate ammonia nitrogen and non-biodegradable and/or toxic organic pollutants from actual wastewaters at laboratory scale [1–4]. In terms of operation and investment costs, BDD electro-oxidation can compete satisfactorily with Fenton oxidation in the treatment of several wastes [5]. Serikawa et al. [6] reported that electrochemical oxidation becomes a cost competitive alternative to other AOPs when the wastewater COD ranges from 1000–30000 mg/L.

Due to the encouraging results obtained at laboratory scale, electro-oxidation of wastewaters by means of BDD anodes has been implemented recently at pilot scale. Anglada et al. [7] described the effect of current density on landfill leachate electro-oxidation and reported on the importance of assessing the interactions that occur between the different species present in the effluent. Urriaga et al. [8] treated landfill leachate by Fenton oxidation followed by electro-oxidation at pilot scale. Although Fenton treatment resulted in 78% COD reduction, it was ineffective towards ammonia oxidation. Further treatment by electro-oxidation brought about the elimination of residual COD and ammonia. Serikawa et al. [6] treated a wastewater with an initial COD concentration of 14000 mg/L at a BDD pilot plant. Complete elimination of COD

was achieved with an energy consumption of 420 kWh/m³ (30 kWh/kgCOD).

In the present work the design of a pilot scale electrochemical reactor with a boron-doped diamond (BDD) on silicon anode is reported. A theoretical model that describes the kinetics of COD oxidation during the electrochemical oxidation of landfill leachate and has been validated at laboratory scale [9] was employed in the scale-up procedure. A pilot plant with a total anode area of 1.05 m² was built and the scale-up procedure was assessed by performing a series of experiments with biologically pre-treated landfill leachate. However, as the electrode gap was smaller in the pilot plant's cells, differences between the reactor's hydrodynamics at laboratory and pilot scale were expected. Since the latter are known to affect the kinetics of pollutant removal [9–12], the disparities caused by the changes in the geometry of the cell had to be quantified and taken into account in the validation of the design equations. Consequently, the mass-transport coefficients, in the laboratory and pilot plant, were determined by the limiting current technique. The resulting values were used to predict the behavior of the system in terms of COD and ammonia oxidation. The latter followed second-order kinetics and could be described by a model previously reported in the literature [7].

2. Materials and Methods

2.1. Materials

The landfill leachate was collected from the municipal landfill site of Meruelo in Cantabria, Spain. The raw leachate was initially

* Corresponding author. Tel.: +34 942201585; fax: +34 942201591.

E-mail address: ortizi@unican.es (I. Ortiz).

Table 1
Characterization of pretreated leachate used as feed in this work and of the effluent of the electro-oxidation process after 8 hours of treatment ($J = 450 \text{ A/m}^2$; $A/V = 1.4$, 4.2 and 7 m^{-1}).

PARAMETER	Influent	Effluent
pH	8.12–9.41	5.37–9.39
Conductivity (mS/cm)	10–10.9	8.1–9.0
Chemical oxygen demand, COD (mgO ₂ /L)	920–1448	n.d.–406
[NH ₄ ⁺] (mg/L)	896–980	n.d.–616
Anion concentrations		
Chloride (mg/L)	1615–1819	250–1656
Nitrite (mg/L)	n.d.–163	n.d.–28
Nitrate (mg/L)	5–1207	529–2849
Sulphate (mg/L)	140–199	124–200

treated *on-site* by a biological process of activated sludge to reduce biodegradable organic compounds and ammonia. The physico-chemical characteristics of the biologically pretreated leachate are shown in Table 1. As it can be seen, the biological process proved to be inefficient. The generated effluent, with a concentration of COD (1100 mg/L) and ammonium (970 mg/L) is above the disposal limits. Also, the landfill leachate presents a high electrical conductivity value, due to the high concentration of chloride anions, permitting the application of electrochemical oxidation without the addition of more electrolytes.

The electrolyte used in the mass transfer measurements consisted of sodium carbonate (Na₂CO₃), potassium ferricyanide [K₃Fe(CN)₆] and potassium ferrocyanide [K₄Fe(CN)₆] (Panreac, Spain). The solutions were prepared using ultrapure water at laboratory scale and rain water stored at the landfill site at pilot plant scale.

2.2. Equipments

2.2.1. Laboratory scale system

The electrochemical cell used in the laboratory was comprised of a circular BDD on silicon anode and a stainless steel cathode with a surface area of 70 cm² each and an inter-electrode gap of 5 mm. Other experimental details can be found in a previous work [9].

2.2.2. Pilot plant scale system

A kinetic model that predicts the evolution of COD with time (Eq. 1) and that had been previously validated at laboratory scale

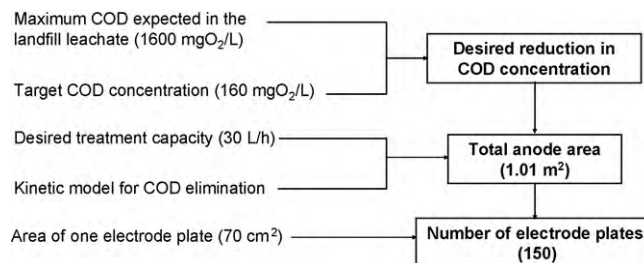


Fig. 1. Overview of the scale-up procedure.

[9] was used as the basis for the scale-up of an electrochemical reactor.

$$COD(t) = COD_0 \exp \left[- \left(\frac{Ak_m}{V} \right) t \right] \quad (1)$$

A basic scheme of the steps that were followed to scale-up the electrochemical reactor is shown in Fig. 1. The quantities on the left hand side are the input parameters, while those on the right hand side are the quantities to be calculated. An electrode area of 1 m² was estimated to be necessary to reduce the concentration of COD, in the biologically-pretreated landfill leachate, from 1600 mg/L to the discharge level into surface water bodies in Spain (160 mg/L) with a treatment capacity of 30L/h. Considering a commercial electrode area of 70 cm², the number of electrodes needed was 150.

The detailed design and construction of the unit was commissioned to Adamant Technologies. In Fig. 2 a schematic diagram of the pilot plant is shown. The elements of the pilot plant can be grouped in three sections: 1) the feeding system, 2) the Diacell unit and 3) the power supply, instrumentation and control unit. The feeding system includes a tank of 750 L and three pumps that continuously feed the electrolyte to be treated into the Diacell unit. In order to maintain the temperature of the process below 35 °C, cooling water is circulated through a refrigeration coil located at the bottom part of the feed tank. Rain water stored at the landfill site is used as cooling water. As the fluid leaves the tank it is distributed in three treatment lines disposed in parallel, with one pump per way. Each pump is able to provide a maximum flowrate of 300 L/min and the minimum flowrate allowed for a DiaCell is 125 L/min per way.

The Diacell unit is divided in three electrochemical lines. Each line consists of five DiaCell sets, containing each set ten DiaCells

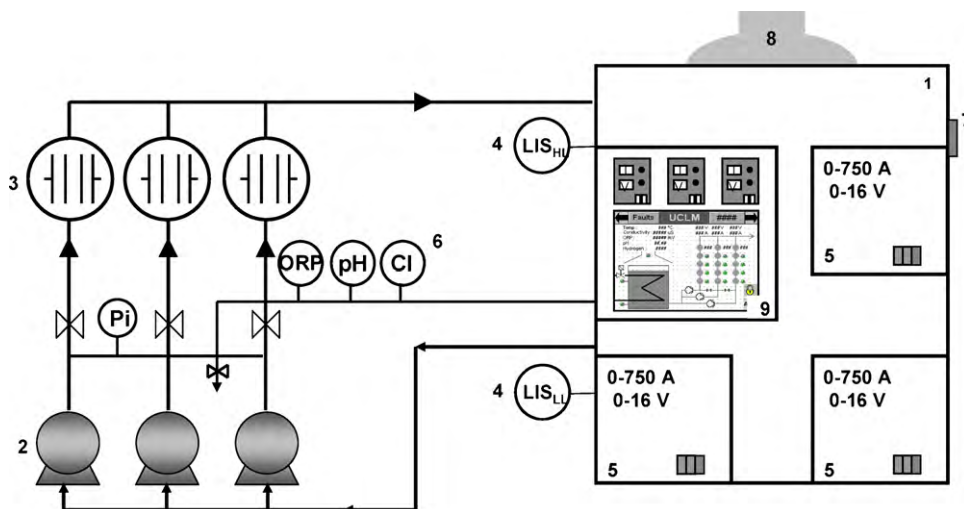


Fig. 2. Schematic diagram of the pilot plant: 1, feed tank; 2, pumps; 3, Diacell unit; 4, low and high level switch; 5, Power rectifiers; 6, Probes; 7, hydrogen sensor; 8, ventilation system; 9, PLC.

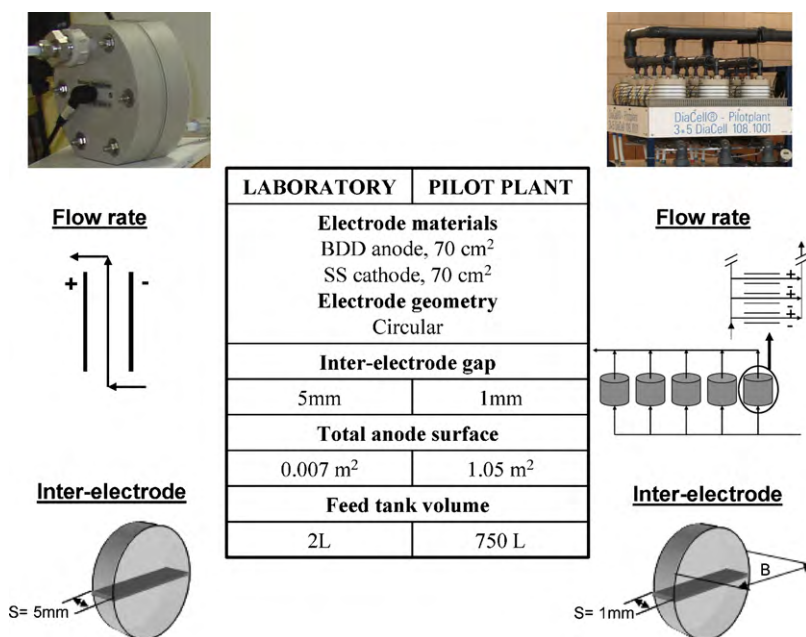


Fig. 3. Parallelisms and differences between laboratory and pilot plant systems.

(anode-cathode pair). This gives a total of 150 DiaCells [10 (Dia-Cell set⁻¹) x (5 sets line⁻¹) x 3 (lines)]. Both the DiaCell packs and the DiaCells are arranged in parallel. The electrode materials are stainless steel for the cathode, and boron-doped diamond (BDD) on silicon as the anode. Their geometry is circular with a useful surface area of 70 cm² each and an electrode gap of 1 mm. The total anode surface is 1.05 m².

Electric power is supplied by three power rectifiers with a maximum output of 750A, 16V. The pilot plant includes also conductivity, temperature, pH and ORP probes which give online measurements, an external hydrogen sensor and a ventilation system. The unit is operated by means of a PLC.

2.3. Analytical determinations

Samples were withdrawn at regular time intervals and preserved in refrigerator at 4°C in accordance with the Standard Methods [13]. Chemical oxygen demand (COD) was determined by closed reflux and colorimetric method (Spectroquant NOVA 400, Merck) following the analytical procedure 5220D from Standard Methods [13]. Ammonium nitrogen concentration was obtained by distillation and titration according to the Standard Method 4500 [13].

2.4. Experiments

Electro-oxidation experiments of landfill leachate at pilot scale were conducted in discontinuous mode. A volume of 250 L of biologically pretreated leachate was treated in each experiment. Landfill leachate was previously ultrafiltrated in a ZeeWeed 10 hollow-fiber membrane module (nominal pore size=0.04 μm, nominal surface area=0.93 m²), to avoid eventual plugging or short-circuit of the electrode compartments. The flow rate was adjusted to 300 L/min per line.

3. Results and discussion

3.1. Mass transfer study

As it can be observed in Fig. 3, the main difference between the DiaCell of the laboratory and pilot plant lies in the inter-electrode

gap value. As the mass-transport coefficient depends on cell geometry and as the inter-electrode gap in the laboratory is five times higher than in the pilot plant, mass transport enhancement is expected at pilot scale. Taking into account that the rate of COD and ammonia oxidation depends on the value of the mass-transport coefficient, it is of paramount importance to quantify the effect of cell geometry on *k_m*.

The average mass-transport coefficient in both laboratory and pilot plant systems was determined using the limiting-current technique. The oxidation of ferrocyanide ion to ferricyanide ion was used as a model reaction to determine *k_m* values in the electrochemical cell. The limiting current was measured over a range of flow rates and temperatures deriving the mass transfer coefficient values at the different operating conditions by Eq. 2 [14].

$$k_m = \frac{I_{lim}}{nFAC_B} \tag{2}$$

To describe the dependence of mass transfer on the fluid properties, hydrodynamics and cell geometry, dimensional analysis has been used (Eq. 3).

$$Sh = aRe^b Sc^c \tag{3}$$

The Reynolds number is defined in Eq. 4 while the linear velocity and equivalent diameter are defined by Eq. 5 and 6, respectively. The latter depends on the cross-flow section of the cell which, in the present study, is a rectangular channel of variable dimensions (BxS) along the fluid circulation path. The geometry of the electrolytic cell is depicted in Fig. 3. In the present work, the minimum Reynolds number that corresponds to the maximum value of B (equal to the diameter of the cell *d*) was considered. Also, the value of the inter-electrode gap, *S_{lab}* = 5 mm and *S_{pp}* = 1 mm, can be considered to be negligible against the electrode diameter, *d* = 94.4 mm. Taking into account the above simplifications, the Reynolds number can be written according to Eq. 7.

$$Re = \frac{ud_e \rho}{\mu} \tag{4}$$

$$u = \frac{Q}{B \cdot S} \tag{5}$$

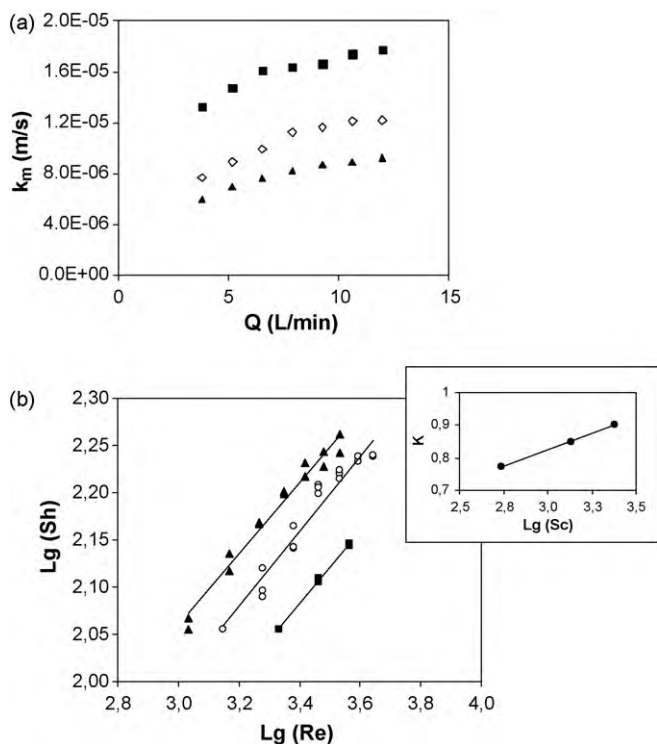


Fig. 4. (a) Influence of flow rate and temperature on the mass transfer coefficient. (b) Log of Sherwood vs. log of Reynolds numbers for experimentally determined mass-transfer coefficients and plot of K vs. $\text{Lg}(Sc)$ (inset). Temperature: \blacktriangle 10 °C, \circ 20 °C, \blacksquare 40 °C.

$$d_e = \frac{2 \cdot B \cdot S}{B + S} \quad (6)$$

$$Re_{\min} = \frac{\rho \cdot Q \cdot 2}{\mu \cdot d} \quad (7)$$

3.1.1. Laboratory scale

In the study performed in the laboratory, the feed tank was charged with 1L of an electrolyte solution containing 0.50 M Na_2CO_3 (supporting electrolyte), 0.05 M $\text{K}_4\text{Fe}(\text{CN})_6$ and 0.10 M $\text{K}_3\text{Fe}(\text{CN})_6$. The influence of the Schmidt group on the mass transfer coefficient was studied by setting the temperature at 10 °C, 20 °C and 40 °C. At each temperature, several experiments were carried out varying the flow rate from 3.8 to 12 L/min. All the experiments were carried out twice in order to check the reproducibility. A detailed description of the procedure followed to carry out the experiments and do the calculations was given by [15].

In Fig. 4a, the influence of flow rate and temperature on the mass-transfer coefficient is shown. It can be seen that high flow rate and temperature values lead to mass-transfer enhancement due to an increase in turbulence and diffusivity respectively. Arranging Eq. 3 in its logarithmic form, Eq. 8 is obtained. For data obtained at the same temperature, the Sc number does not vary, and the terms $\log a$ and $c \log Sc$ can be gathered in a single constant parameter, K (Eq. 9),

$$\log Sh = \log a + b \log Re + c \log Sc \quad (8)$$

$$K = \log a + c \log Sc \quad (9)$$

In Fig. 4b, the linear fitting of the experimental data to eqs. 8 and 9 is shown. It can be observed that the data, expressed in terms of Sh against Re and Sc , are well fitted by equation 3 if values of $a = 1.67$, $b = 0.385$ and $c = 0.2$ are considered (Eq. 10). Over the range of Reynolds numbers for which experiments were conducted (2100–6700), b and c values in the range 0.36–0.875 and 0.21–0.33,

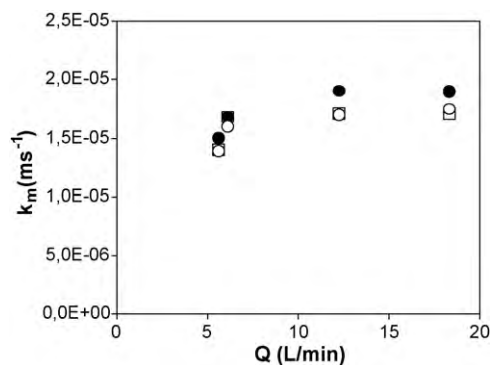


Fig. 5. Influence of flow rate on the mass-transfer coefficient in each line of the pilot plant. Line: \square line 1, \bullet line 2, \circ line 3.

respectively, have been reported in the literature for flat parallel electrodes [16–18]. Consequently, the values of parameters b and c are in agreement with the lower range values previously reported in the literature.

$$Sh_{lab} = 1.67 Re^{0.385} Sc^{0.20} \quad (10)$$

3.1.2. Pilot scale

In order to determine the mass-transport coefficient, the same procedure employed at laboratory scale was followed in the pilot plant. The electrolyte employed in this set of experiments had the same characteristics as the electrolyte used in the laboratory. Two hundred and fifty liters of the electrolyte solution were freshly prepared before the experiment. However, in this case only the relationship between the mass-transport coefficient and flowrate was experimentally studied. The runs were carried out at a temperature of 20 °C, while the flowrate through each electrochemical cell ranged from 5.6 to 18.3 L/min (Re : 2150–7030). Each line of the pilot plant was tested individually. In Fig. 5, the variation of mass-transfer coefficient with flow rate is shown. It can be observed that flow rate had a lower effect on the mass-transfer coefficient than that observed in the laboratory system and that all lines showed the same behaviour.

As already stated, the main difference between the electrolytic cells used in the laboratory and pilot plant lies in the distance between electrodes, a geometrical characteristic that is expected to affect the value of the pre-exponential parameter a [10]. For this reason, the mass transfer coefficients k_m obtained from the limiting-current experiments in the pilot plant were fitted using the same values of the parameters b and c obtained at lab scale, determining only a . The data obtained in the pilot plant were satisfactorily described by a value of a equal to 0.54 (Eq. 11),

$$Sh_{pp} = 0.54 Re^{0.385} Sc^{0.20} \quad (11)$$

A plot of the experimental Sherwood versus the theoretical predictions obtained using eqs. (10) and (11) is shown in Fig. 6. Good agreement between the modelled and experimental data is observed as the simulated Sh values fall within the experimental Sh range $\pm 10\%$.

If the expressions for the Sherwood, Schmidt and Reynolds number are substituted in equations 10 and 11 and the correlation between the mass-transport coefficient in the pilot plant and in the laboratory is calculated, the following expression is obtained:

$$\frac{k_{m,lab}}{k_{m,pp}} = \frac{a_{lab}}{a_{pp}} \cdot \left(\frac{Q_{lab}}{Q_{pp}}\right)^b \cdot \left(\frac{S_{pp}}{S_{lab}}\right) = 062 \cdot \left(\frac{Q_{lab}}{Q_{pp}}\right)^{0.385} \quad (12)$$

In equation 12 it can be clearly seen that for a given flow rate, the mass transport coefficient in the laboratory is lower than in the pilot plant due to its higher inter-electrode gap.

Table 2
Initial composition of the biologically treated landfill leachate and operation conditions used in the experiments performed at pilot scale.

Exp	A/V (m ⁻¹)	J _{appl} (A/m ²)	COD ₀ (mg/L)	[NH ₄ ⁺] ₀ (mg/L)	[Cl ⁻] ₀ (mg/L)
1,2,3	1.4	450	960	905	1700
4,5,6	4.2	450	960	905	1700
7,8,9	7	450	1448	980	1820

3.2. Scale-up of COD oxidation

In the laboratory, 1L of biologically pre-treated leachate was electro-oxidized in a cell with an anode area of 70 cm² (A/V = 7 m⁻¹). Then, a set of experiments was conducted at pilot scale in which the “total anode area/volume of the effluent to be treated ratio (A/V)” was modified. In the *Materials and Methods* section, it was explained that the pilot plant is comprised of three treatment lines disposed in parallel, with an anode area of 0.35 m² per way. Thus, to modify the A/V ratio, the following procedure was followed. First, each line was operated individually and in each case 250 L of biologically pre-treated landfill leachate were electrochemically oxidized at a current density of 450 A/m². The flow rate was adjusted to 300 L/min per line or 6 L/min per Diacell. Secondly, another experiment was performed in which all three lines were operated simultaneously. Thus, the A/V ratio was 1.4 m⁻¹ (0.35 m²/0.25 m³) when each line was operated individually and 4.2 m⁻¹ (1.05 m²/0.25 m³) when all three lines were operated simultaneously. The operating conditions under which these experiments were performed are shown in Table 2.

In Fig. 7a, the COD concentration profiles for an A/V ratio of 1.4 m⁻¹ are compared with the results obtained when an A/V ratio of 4.2 m⁻¹ and 7 m⁻¹ (laboratory scale, 0.007 m²/0.001 m³) is employed. It should be pointed out, that the three electrochemical lines (A/V= 1.4 m⁻¹) had the same behaviour -similar COD concentration profiles were obtained with an experimental error lower than 9.5%- and average values are represented in Fig. 7a. Comninellis’ model (Eq.1) was used to predict the experimental results. To do this, equations 10 and 11 were used to estimate the mass-transfer coefficients in the laboratory and pilot plant, respectively, obtaining the following values: $k_{m,pp} = 1.6 \times 10^{-5} \text{ ms}^{-1}$; $k_{m,lab} = 1.2 \times 10^{-5} \text{ ms}^{-1}$. Simulated profiles are also plotted in Fig. 7a and are represented by solid lines. As it can be observed, the increase in the COD oxidation rate could be well predicted by equations 1, 8 and 9 with standard deviations between experimental data and simulated values ranging from 4.4 to 9%.

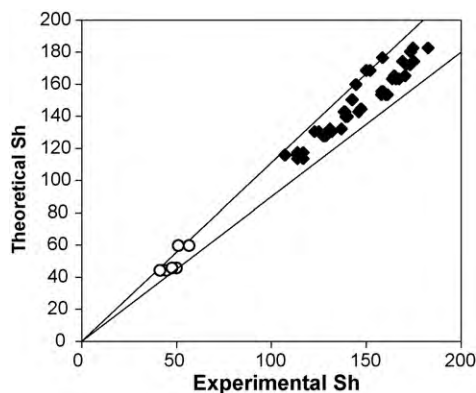


Fig. 6. Plot of experimentally determined Sherwood number versus the values calculated using the best-fit *a*, *b* and *c* parameters at □ lab and ■ pilot scale.

3.3. Scale-down of NH₃ oxidation

In the above mentioned experiments, the evolution of NH₃ concentration with treatment time was also determined (Fig. 7b). However, in this case, a model (Eq.13–15) that had been previously developed at pilot scale [7] was used to predict the data obtained with the different A/V ratios. The model considers that ammonia oxidation occurs through indirect oxidation mechanisms by means of electro-generated active chlorine. During indirect oxidation of ammonia, chlorine evolution occurs at the anode. At pH < 3.3, aqueous chlorine is the predominant species whereas at higher bulk pH values, its diffusion away from the anode is coupled to its dismutation reaction to form hypochlorous acid at pH < 7.5 and hypochlorite ions at pH > 7.5. Then, HOCl reacts with NH₃ through breakpoint chlorination reactions to regenerate chloride ions.

$$\frac{d[\text{NH}_4^+]}{dt} = -k \cdot [\text{NH}_4^+] \cdot [\text{“Cl}_2\text{”}] \quad (13)$$

$$\frac{d[\text{“Cl}_2\text{”}]}{dt} = \frac{\phi j A}{n F V} \quad (14)$$

$$\ln \frac{[\text{NH}_4^+]}{[\text{NH}_4^+]_0} = -\frac{k \phi j A t^2}{4 n F V} = -k' t^2 \quad (15)$$

In the previous study [7], the effect of current density on ammonia oxidation was assessed and an empirical equation that described the dependency of the kinetic parameter *k'* on the applied

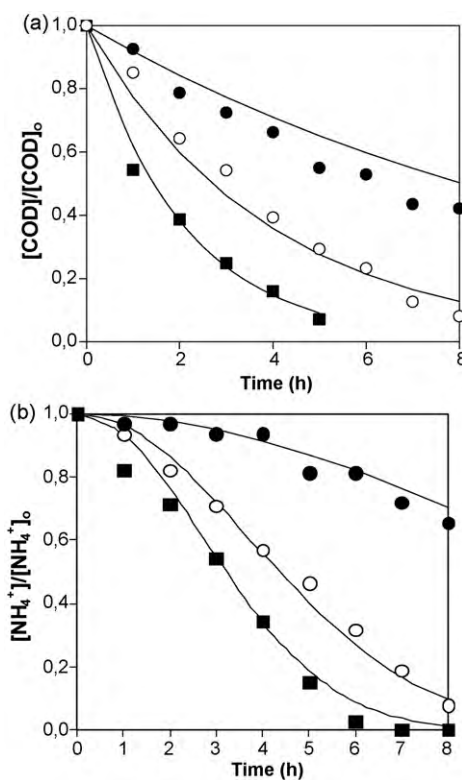


Fig. 7. Normalized COD (a) and NH₄⁺ (b) concentration profiles. ● A/V= 1.4 m⁻¹; ○ A/V= 4.2 m⁻¹; ■ A/V= 7 m⁻¹. Solid lines represent simulated data obtained by the mathematical models. Applied current density: 450A/m².

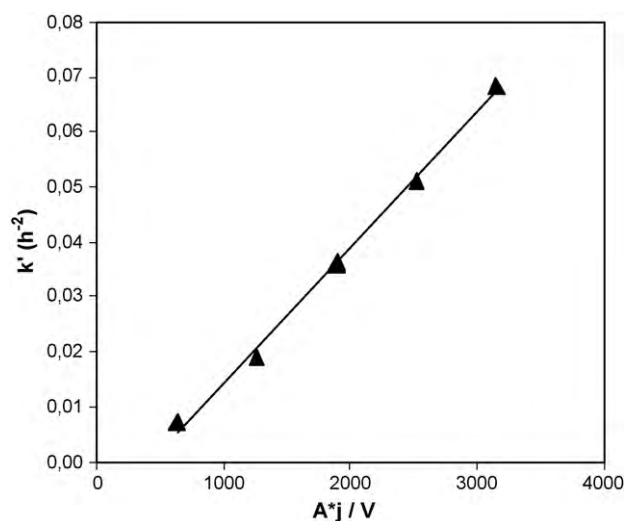


Fig. 8. Linear fitting of $k'(h^{-2})$ values vs $A \times j/V$.

current density was obtained (Eq. 16). In contrast to what was expected from equation 15, equation 16 did not pass through the origin. This was explained on the basis that at low current densities, oxidation of organic matter takes place primarily at the anode surface pushing chlorine evolution and thus ammonia oxidation into the background.

$$k' = 1.07 \cdot 10^{-4} \cdot j - 1.292 \cdot 10^{-2} (h^{-2}) \quad (16)$$

It should be highlighted that equation 16 is valid for an A/V ratio of $4.2 m^{-1}$ and for current densities in the range 300–600 A/m^2 . Consequently, equation 16 has to be rewritten in order to take into account the change of scale that influences the A/V ratio. For this purpose, values of k' were calculated from the slopes of the $\ln([NH_4^+]/[NH_4^+]_0)$ vs the square of electrolysis time for the different A/V ratios employed, both in the laboratory and pilot plant, and were represented together with those obtained in the previous study in Fig. 8. It can be observed that the value of k' increased linearly with the applied current density and A/V ratio and that, as in equation 16, the linear regression did not pass through the origin. The empirical equation obtained via a linear fitting of the data shown in Fig. 8 is:

$$k' = 2.45 \cdot 10^{-5} \cdot \left(\frac{A \cdot j}{V}\right) - 0.00994 (h^{-2}) \quad (R^2 = 0.996) \quad (17)$$

The comparison between the experimental ammonium concentration profiles and the ammonium concentration predicted by the revised empirical model (Eqs. (15) and (17)), which takes into account changes in the volume of effluent treated and available anodic area, is shown in Fig. 7b. The model satisfactorily predicts ammonia removal during electrochemical oxidation of biologically treated leachate, with standard deviations between the experimental and simulated results ranging from 8.9 to 10.5%.

3.4. Nitrate formation and energy consumption

Several properties besides ammonia and COD concentration were analyzed during the electro-oxidation experiments. In Table 1, the range within which each parameter varied in the effluent obtained after 8 hours of treatment in experiments 1 to 9 is shown. It can be observed that, under appropriate conditions, electro-oxidation was capable of eliminating COD and ammonia completely. However, as a result of ammonia oxidation, the concentration of nitrate ions which was initially high was further increased. The percentage of $N-NH_4^+$ oxidized to $N-NO_3^-$ ranged

from 44% to 63%. Consequently, although the electro-oxidation process was able to control COD and ammonia within the discharge standards, the final effluent did not match the discharge standard with respect to nitrate concentration. In previous studies, deployment of electrochemical oxidation in combination with ion exchange [19] or reverse osmosis [20] as a post-treatment step was proposed as a possible solution to this issue.

As electricity is basically the only consumable in electrochemical oxidation, its efficiency is usually assessed in terms of specific energy consumption. This is defined as the amount of energy consumed per unit mass of pollutant load removed. The specific energy consumption required to reduce the concentration of COD below the discharge limit of 160 mg/L was 94 kWh/kgCOD when 250 L of landfill leachate were treated at 450 A/m^2 . This value can be lowered to 53 kWh/kgCOD by bringing the current density down to 300 A/m^2 [21]. Further information regarding the economic feasibility of BDD electro-oxidation of landfill leachate can be found in a recent study [21] in which this technology was compared with other commonly used AOPs such as Fenton treatment.

4. Conclusions

In this work, the importance of properly describing the electrochemical cell's hydrodynamics was demonstrated. Generalized dimensionless correlations regarding mass transfer were developed in order to define the mass transfer conditions in a laboratory and pilot scale electrochemical system. The former had an anode area of 70 cm^2 while the latter of 1.05 m^2 . Then, the mass-transfer coefficients calculated were used to predict the results obtained, in terms of COD and ammonia removal, during electrochemical oxidation of biologically pre-treated landfill leachate. For this purpose, two mathematical models that had been previously used to describe organic matter and ammonia electro-oxidation kinetics were used. Good agreement between the experimental and simulated data was obtained. As far as the model that describes ammonia oxidation is concerned, the pseudo-kinetic constant had to be re-defined in order to take into account its dependence on the anodic area/volume treated, A/V , ratio.

Nomenclature

A	electrode surface area (m^2)
C_B	concentration of ferrocyanide ions ($mol m^{-3}$)
B	width of cell or cell channel (m)
S	interelectrode distance (m)
d_e	cell equivalent diameter (m)
F	Faraday constant ($96485 C mol^{-1}$)
n	electrons exchanged in electrode reaction
I_{lim}	limiting current value (A)
k_m	mass-transfer coefficient (ms^{-1})
Sh	Sherwood number based on cell equivalent diameter ($k_m d_e / D$)
Re	Reynolds number ($d_e v \rho / \mu$)
Sc	Schmidt number ($\mu / \rho D$)
u	velocity (ms^{-1})
Q	flow rate ($m^3 s^{-1}$)
ρ	fluid density ($kg m^{-3}$)
μ	dynamic viscosity ($kgs^{-1} ms^{-1}$)
$[Cl_2]$	concentration of dissolved active chlorine
$[NH_4^+]$	concentration of ammonia
k	second-order rate constant ($mol^{-1} s^{-1}$)
V	volume of effluent treated (m^3)
Φ	current efficiency for chlorine evolution
j	applied current density (Am^{-2})

Acknowledgments

Financial support of projects CTM2006-00317, CTQ2008-00690 is gratefully acknowledged. A. Anglada would like to thank the Spanish Ministry of Innovation and Science (MICINN) for a FPU research grant.

References

- [1] A. Cabeza, A. Urriaga, M.J. Rivero, I. Ortiz, Ammonium removal from landfill leachate by anodic oxidation, *J. Hazard. Mater.* 144 (2007) 715–719.
- [2] E. Chatzisymeon, N. Xekoukoulotakis, E. Diamadopoulos, A. Katsaounis, D. Mantzavinos, Boron-doped diamond anodic treatment of olive mill wastewaters: Statistical analysis, kinetic modeling and biodegradability, *Water Res.* 43 (2009) 3999–4009.
- [3] P. Cañizares, A. Beteta, C. Sáez, L. Rodríguez, M.A. Rodrigo, Use of electrochemical technology to increase the quality of the effluents of bio-oxidation processes. A case studied, *Chemosphere.* 72 (2008) 1080–1085.
- [4] A. Anglada, A. Urriaga, I. Ortiz, Contributions of electrochemical oxidation to waste-water treatment: fundamentals and review of applications, *J. Chem. Technol. Biot.* 84 (2009) 1747–1755.
- [5] P. Cañizares, R. Paz, C. Sáez, M.A. Rodrigo, Costs of the electrochemical oxidation of wastewaters: a comparison with ozonation and Fenton oxidation processes, *J. Environ. Manage.* 90 (2009) 410–420.
- [6] R.M. Serikawa, Y. Senda, K. Sasaki, Industrial E-AOP application using boron doped diamond electrodes, in: *Proceedings of AOP5*, held in Berlin, Germany, 2009.
- [7] A. Anglada, A. Urriaga, I. Ortiz, Pilot scale performance of the electro-oxidation of landfill leachate at boron-doped diamond anodes, *Environ. Sci. Technol.* 43 (2009) 2035–2040.
- [8] A. Urriaga, A. Rueda, A. Anglada, I. Ortiz, Integrated treatment of landfill leachates including electrooxidation at pilot plant scale, *J. Hazard. Mater.* 166 (2009) 1530–1534.
- [9] A. Cabeza, A.M. Urriaga, I. Ortiz, Electrochemical treatment of landfill leachates using a boron-doped diamond anode, *Ind. Eng. Chem. Res.* 46 (2007) 1439–1446.
- [10] H. Wendt, G. Kreysa, *Electrochemical engineering: science and technology in chemical and other industries*, Springer, Germany, 1999.
- [11] K. Jüttner, U. Galla, H. Schmieder, Electrochemical approaches to environmental problems in the process industry, *Electrochim. Acta.* 45 (2000) 2575–2594.
- [12] A. Kapalka, G. Fóti, C. Comninellis, Basic principles of the electrochemical mineralization of organic pollutants for wastewater treatment, in: C. Comninellis, G. Chen (Eds.), *Electrochemistry for the Environment*, Springer, New York, 2009, pp. 1–25.
- [13] *Standard Methods for Examination of Water and Wastewater*, 20th Edition; American Public Health Association (APHA): Washington, DC, 1998.
- [14] C.F. Oduoza, A. Wragg, Effects of baffle length on mass transfer in a parallel plate rectangular electrochemical cell, *J. Appl. Electrochem.* 30 (2000) 1439–1444.
- [15] P. Cañizares, J. García-Gómez, I. Fernández de Marcos, M.A. Rodrigo, J. Lobato, Measurement of mass-transfer coefficients by an electrochemical technique, *J. Chem. Educ.* 83 (2006) 1204–1207.
- [16] D.J. Pickett, B.R. Stanmore, Ionic mass transfer in parallel plate electrochemical cell, *J. Appl. Electrochem.* 2 (1972) 151–156.
- [17] T.R. Ralph, M.L. Hitchman, J.P. Millington, F.C. Walsh, Mass transport in an electrochemical laboratory filterpress reactor and its enhancement by turbulence promoters, *Electrochim. Acta.* 41 (1996) 591–603.
- [18] N. Tzanetakis, K. Scott, W.M. Taama, R.J.J. Jachuck, Mass transfer characteristics of corrugated surfaces, *Appl. Therm. Eng.* 24 (2004) 1865–1875.
- [19] A. Cabeza, O. Primo, A.M. Urriaga, I. Ortiz, Definition of a clean process for the treatment of landfill leachates integration of electrooxidation and ion exchange technologies, *Sep. Sci. Technol.* 42 (2007) 1585–1596.
- [20] A. Cabeza, A.M. Urriaga, I. Ortiz, Eco-friendly treatment of landfill leachates by electrochemical oxidation, in: *Proceedings of the 1st International Congress on Green Process Engineering*, Toulouse, France, 2007.
- [21] A. Anglada, D. Ortiz, A.M. Urriaga, I. Ortiz, Electrochemical oxidation of landfill leachates at pilot scale: evaluation of energy needs, *Water Sci. Technol.* 61 (2010) 2211–2217.